

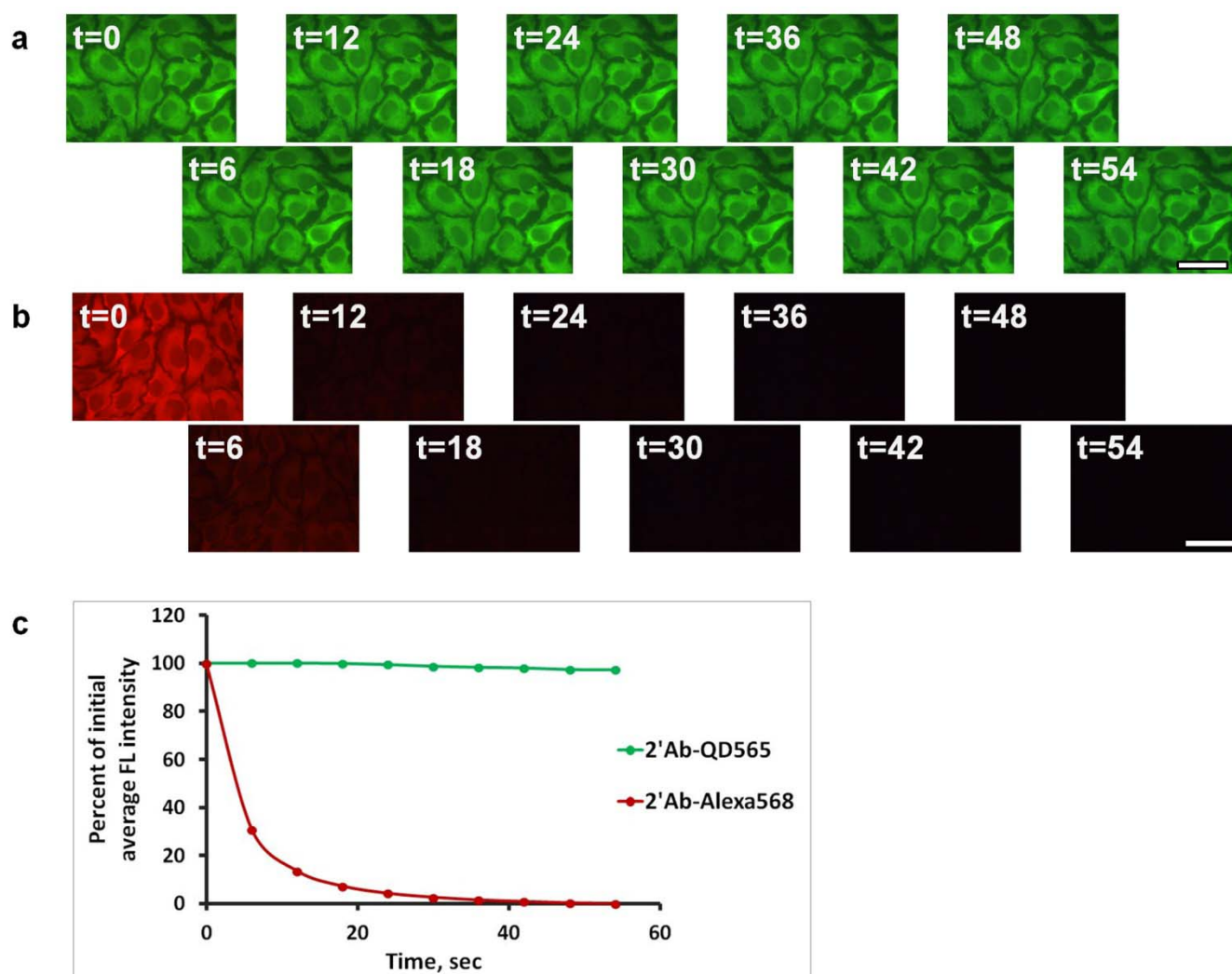
## **Supplementary Information**

### **Quantum Dot Imaging Platform for Single-Cell Molecular Profiling**

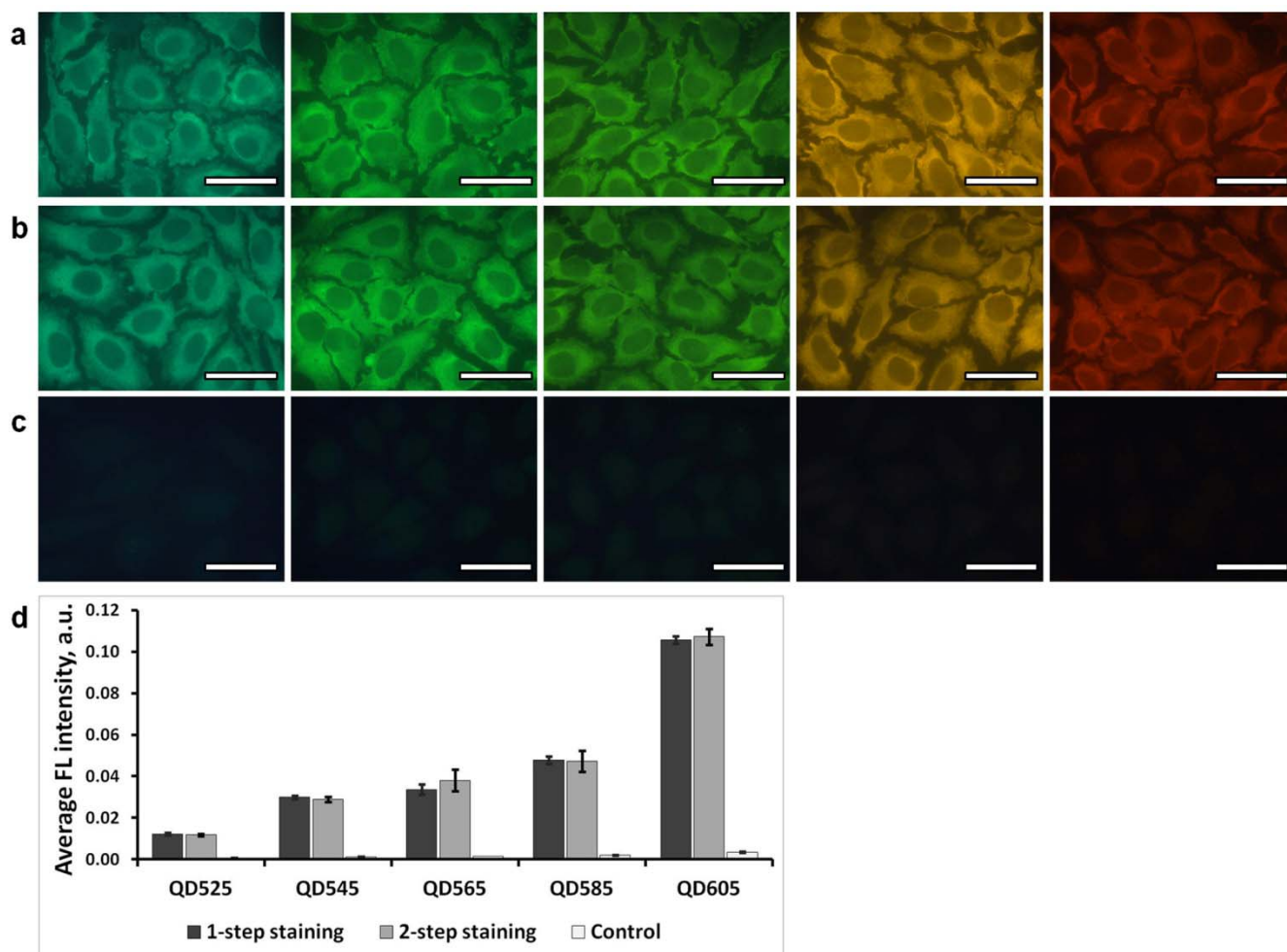
**Pavel Zrazhevskiy and Xiaohu Gao\***

Department of Bioengineering, University of Washington, Seattle, WA 98195, USA.

Correspondence and requests for materials should be addressed to X.H.G. (email: [xgao@uw.edu](mailto:xgao@uw.edu)).

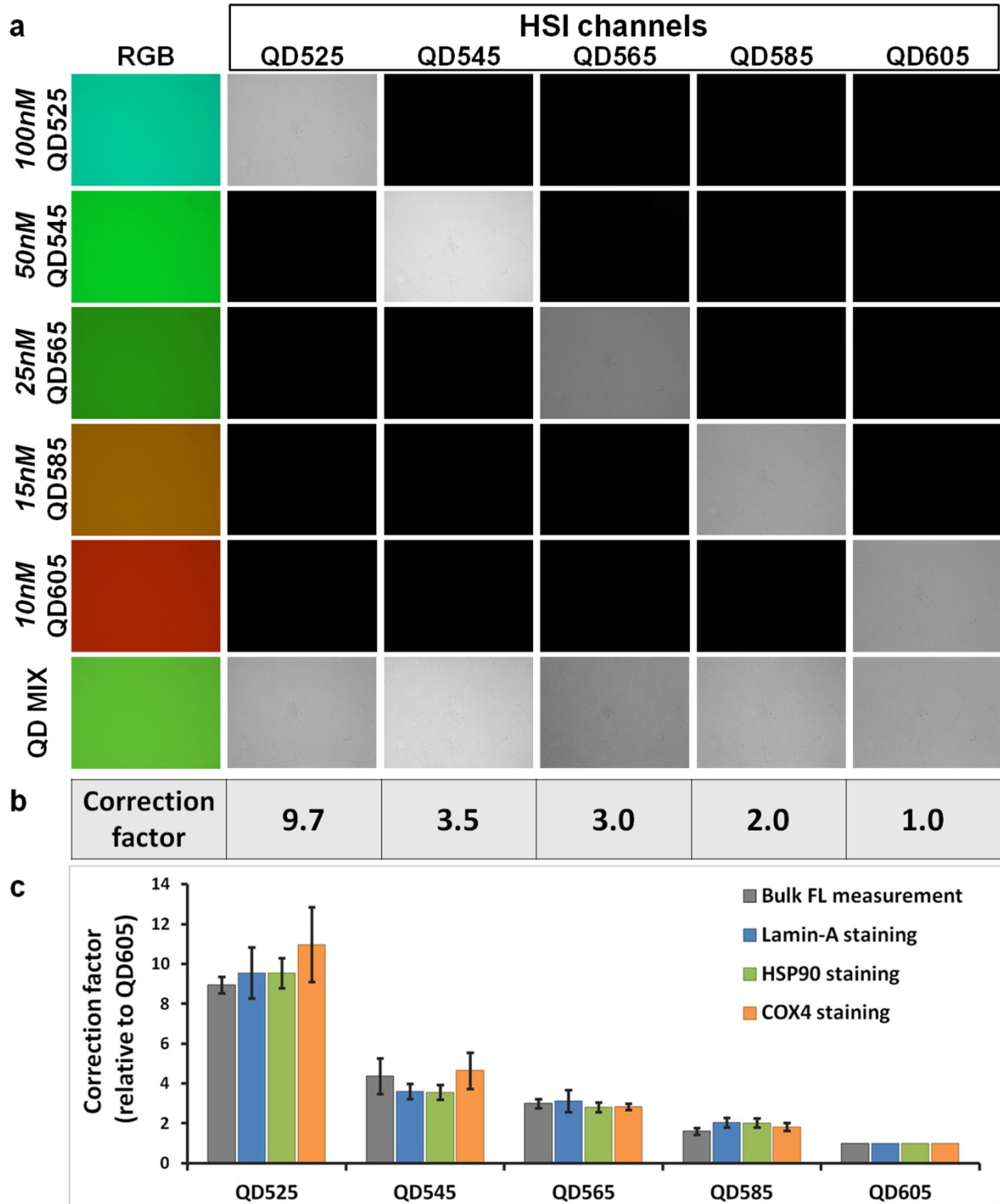


**Supplementary Figure S1. Superior photostability of QD probes in comparison to organic fluorophores.** HSP90 is stained in fixed HeLa cells via a 2-step procedure using anti-HSP90 1'Ab and either matching QD565-labeled 2'Ab (a) or Alexa Fluor 568-labeled 2'Ab (b). Continuous imaging of QD-labeled specimen for 1 minute reveals lack of staining intensity fluctuation (a,c) enabling robust image acquisition and consistent quantitative analysis of staining intensity. In contrast, continuous imaging of Alexa Fluor 568-labeled cells shows quick photobleaching of the dye (b,c), which reduces useful timeframe for image acquisition and severely hampers quantitative signal analysis. Scale bar, 50 $\mu$ m.



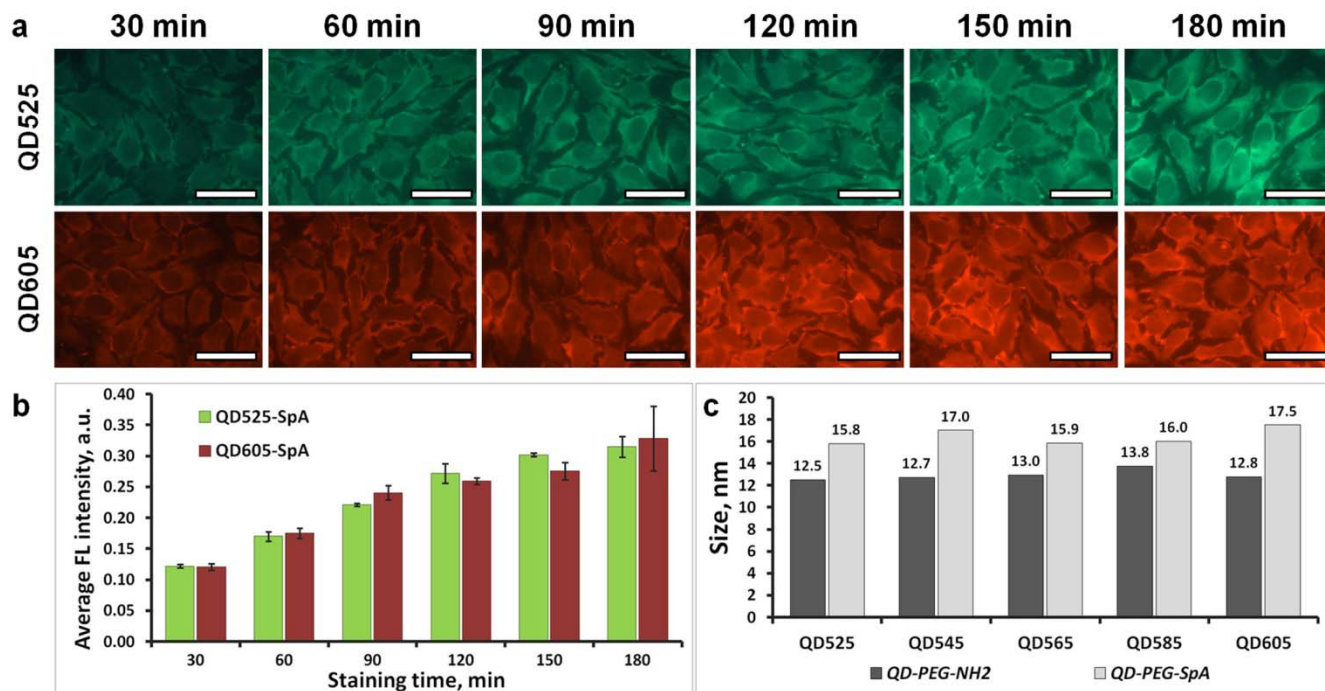
**Supplementary Figure S2. Validation of SpA-mediated QD-Ab probe assembly and staining stoichiometry.** As illustrated in the probe design, QD-SpA-Ab bioconjugates are formed via non-covalent binding between SpA and Ab. However, direct interaction between QDs and Abs via other routes (*e.g.*, electrostatic or hydrophobic interactions) might also be possible. To confirm that the assembly is indeed due to SpA-IgG binding, we performed a series of control staining experiments. First, all 5 different QD-SpA conjugates (emission maxima, from left to right, 525, 545, 565, 585, and 605 nm) are used in 1-step staining of HSP90, showing consistent cytoplasmic localization of this target (a) and indicating that QD-SpA-Ab complex has formed successfully. Second, 2-step HSP90 staining is performed by first incubating cells with 1'Ab targeting HSP90, then labeling with QD-SpA. Consistent cytoplasmic staining with similar signal intensity is obtained in this case as well (b), confirming that QD-SpA probes recognize target-bound 1'Abs inside cells. Third, control staining with QD-SpA probes (no Ab) shows virtually no labeling (c). Taken together, these experiments unambiguously show that the

QD-SpA-Ab complex formation is mediated exclusively by SpA-Ab binding. Furthermore, since at most one QD-SpA can bind to a target-bound Ab in a 2-step procedure, and consistent staining intensity is obtained with both 1-step and 2-step procedures (**d**), these results indicate that QD-SpA-Ab probes produce cell staining in a stoichiometric manner. Consistent imaging parameters were used for each QD color to aid in direct comparison of staining intensity. Error bars represent standard deviation of the average staining intensity between 3 different fields of view imaged on the same specimen. Scale bar, 50 $\mu$ m.

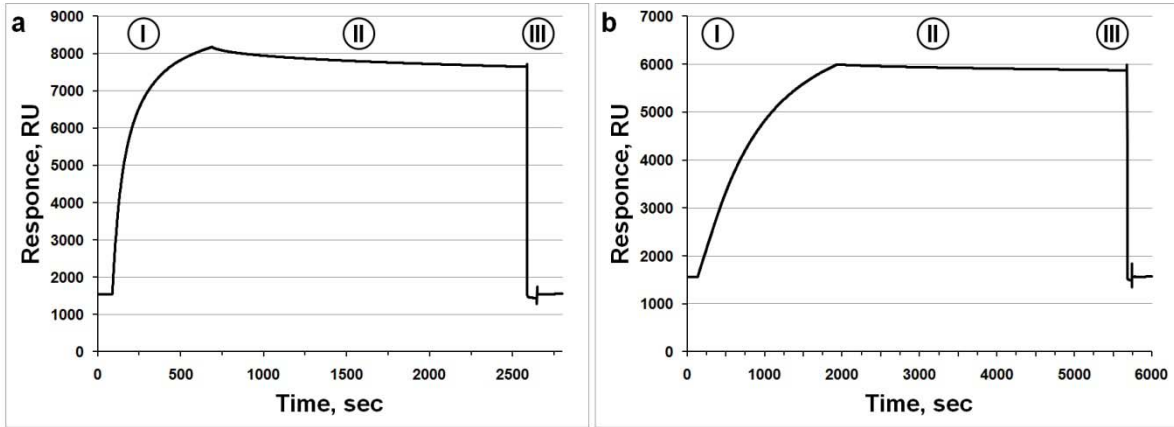


**Supplementary Figure S3. Quantitative evaluation of cell staining with QD-SpA-Ab probes.** Due to narrow symmetrical QD emission profiles, HSI is capable of separating individual signals of QDs with emission peaks

spaced as close as 20 nm apart, yielding lack of spectral crosstalk between QD channels and enabling accurate quantitative measurement of individual QD probe intensities **(a)**. Since different QD probes exhibit varying fluorescence brightness under identical imaging conditions (mostly due to varying quantum yield and light absorption efficiency), bulk fluorescence measurements of QDs in solution are performed with HSI to determine differential brightness and establish correction factors for quantitative comparison of staining intensity obtained with different QD probes **(b)**. Accuracy of such correction factors and consistency of labeling of various intracellular targets are confirmed by separately staining 3 different molecular targets (Lamin A, HSP90, and Cox4) with all 5 QD colors in a singleplexed format and independently comparing differential QD brightness obtained from cell staining with bulk fluorescent measurements **(c)**. Error bars represent standard deviation of average signal intensity between 3 different fields of view imaged for cell staining and between 3 different experiments for bulk fluorescence measurements. Note, that variations in imaging instrumentation (*e.g.* different excitation source, wavelength-dependent camera sensitivity) might also affect measured relative QD brightness. Therefore, assessment of differential QD brightness should be done for each QD-SpA probe batch and for each imaging setup used for quantitative analysis.

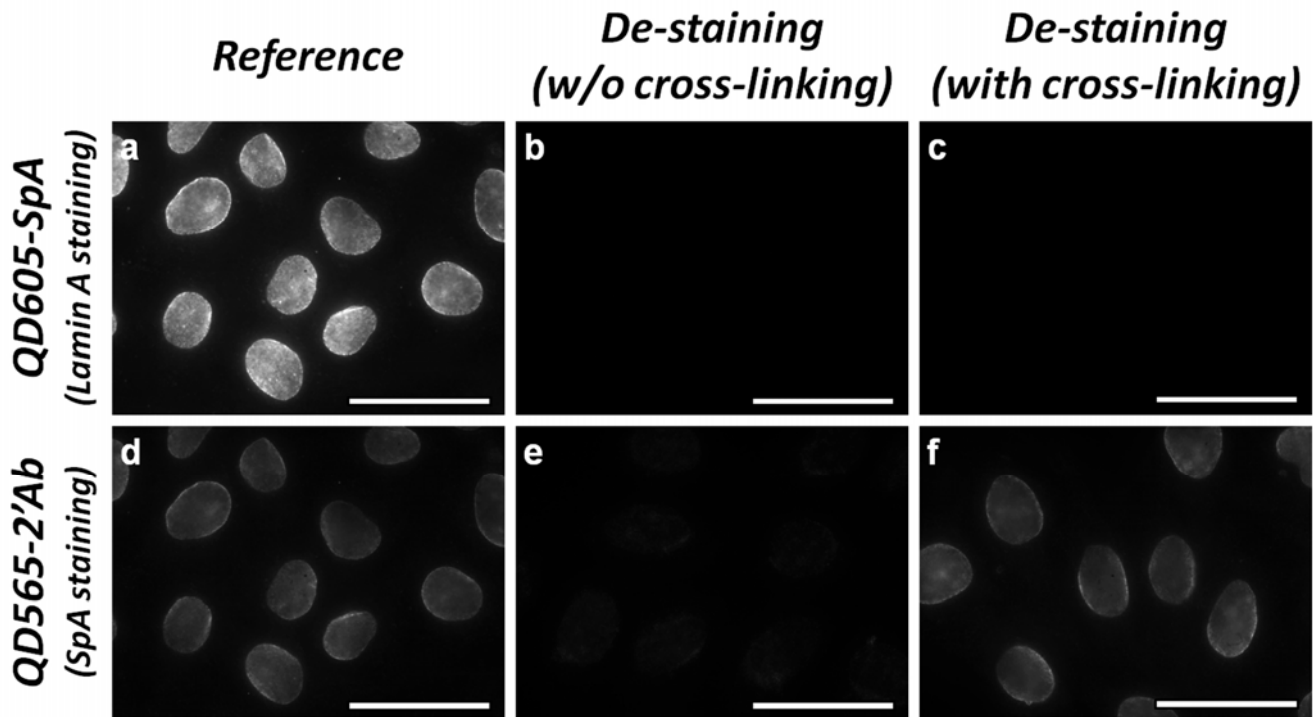


**Supplementary Figure S4. Evaluation of staining kinetics with QD-SpA-Ab probes.** HSP90 is stained in 12 separate specimens by either QD525-SpA-Ab (smallest inorganic core) or QD605-SpA-Ab (largest inorganic core) probes (a). Staining is allowed to proceed for 30, 60, 90, 120, 150, or 180 minutes before specimens are washed and imaged. Both probes demonstrate comparable staining specificity and evolution of signal intensity with increasing incubation time. HSI-based quantitative analysis shows steady increase in staining intensity through the first 2 hours of incubation, mostly reaching a plateau at longer time (b). Error bars represent standard deviation of the average staining intensity between 3 different fields of view imaged on the same specimen. Scale bar, 50 $\mu$ m. Importantly, regardless of staining duration both probes produce nearly identical signal intensity, yielding consistent staining kinetics (note, QD525 signal is adjusted by a correction factor of 9.7 for direct comparison with QD605). Such behavior stems from the similar hydrodynamic size (and thus diffusion kinetics) of all QD-SpA probes - while inorganic core size of different QDs varies substantially, overall hydrodynamic size of PEG-coated water-soluble QDs, being mostly defined by various organic coatings rather than by the core size, remains similar (c, dark bars). Further functionalization with SpA results in slight QD size increase, but does not introduce disparity in sizes of different QD-SpA probes, offering uniform staining kinetics throughout all QD probes used (c, light bars). Hydrodynamic size (diameter) was measured by dynamic light scattering for QDs suspended in TBS at 1 $\mu$ M final particle concentration.

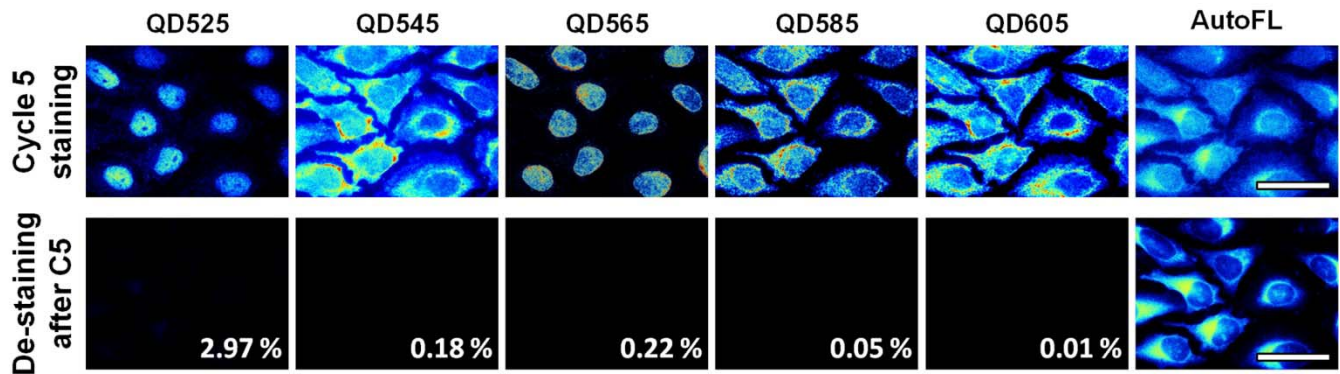


**Supplementary Figure S5. SPR analysis of SpA-Ab bond stability.** Binding (phase I) and dissociation (phase II) of free rabbit anti-mouse IgG to SpA immobilized on the surface of C5 chip is monitored. **(a)** At 100nM Ab concentration fast saturation of surface binding sites during binding phase and quick initial dissociation of Ab followed by a very slow dissociation kinetics during dissociation phase can be observed. **(b)** At 10nM Ab concentration only slow dissociation can be observed, yielding an overall retention of >97% bound Ab after 1 hour of washing. Phase III represents chip surface regeneration with low-pH buffer.

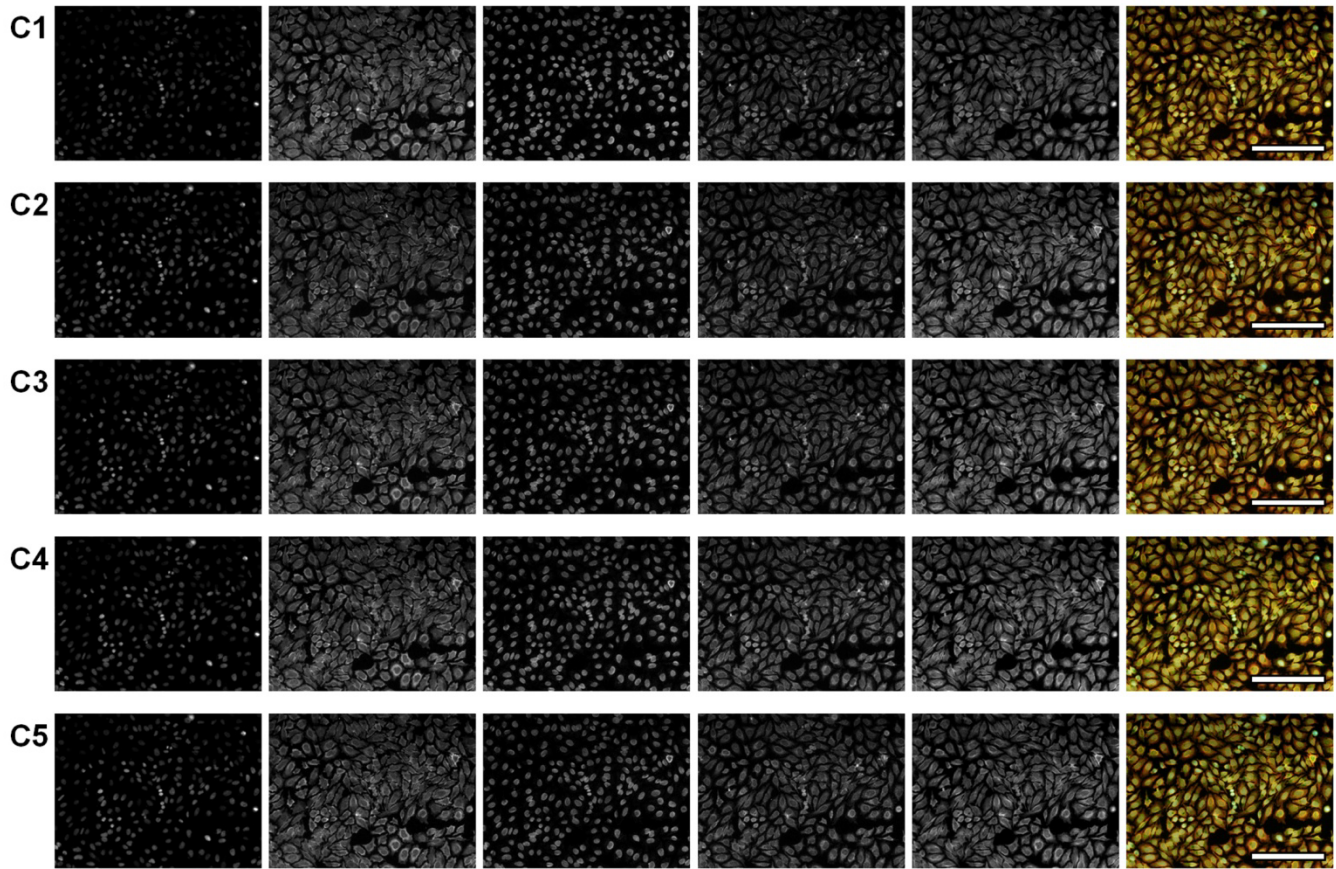




**Supplementary Figure S6. Confirmation of complete specimen regeneration during low-pH/detergent-mediated de-staining.** Lamin A staining with QD605-SpA-Ab probe shows characteristic nuclear envelope staining pattern in QD605 spectral channel (**a**). At the same time, presence of QD-SpA probes can be detected by further staining of SpA using anti-SpA Ab (mouse anti-SpA IgG, Sigma Aldrich) and anti-mouse QD565-2'Ab (**d**). After de-staining QD605 signal is completely eliminated (**b**), while barely detectable QD565 staining of SpA highlights trace amounts (< 10%) of leftover QD605-SpA probes (**e**), indicating that majority of QD-SpA probes are efficiently eluted from the specimen, whereas remaining probes are completely quenched. In contrast, post-staining crosslinking of QD-SpA-Ab probes to specimen hinders elution, as indirectly evidenced by preserved SpA staining in QD565 channel (**f**), keeping all QD-SpA-Ab probes attached to the specimen. Yet, even in this case QD605 signal is completely eliminated following de-staining (**c**), proving low-pH-mediated QD quenching as a sufficient method for elimination of non-specific fluorescence background build-up through staining cycles. Brightness of all images is normalized to (**a**) to facilitate in direct comparison of staining intensity. Scale bar, 50 $\mu$ m.



**Supplementary Figure S7. Verification of the lack of QD fluorescence signal carry-over through 5 cycles of 5-color staining.** To confirm complete specimen regeneration and removal of all QD signal by a de-staining step through multiple cycles of M3P procedure, a set of 5 model molecular targets (Ki-67, HSP90, Lamin A, Cox-4, and  $\beta$ -tubulin) is re-labeled with a library of matching QD-SpA-Ab probes (emitting at 525, 545, 565, 585, and 605 nm respectively) through 5 cycles (see Figure 6 for a full set of images). After the 5th cycle, cells are once again de-stained, and the same sub-set of cells is analyzed with HSI. To facilitate direct comparison of fluorescence signal intensities, unmixed cell images obtained after cycle 5 staining (**top row**) and consequent de-staining (**bottom row**) are presented. Signal intensity within each individual QD channel (columns QD525 through QD605) as well as cell autofluorescence channel (column AutoFL) are normalized and false-colored with a heat map. Residual signal intensity after de-staining is indicated as a % fraction of the Cycle 5 staining intensity within each QD channel. Qualitative and quantitative analysis of cell imaging data unambiguously demonstrates complete removal of the QD signal during de-staining step. At the same time specimen autofluorescence remains nearly unaffected, outlining preserved cell morphology. Slightly higher levels of residual fluorescence detected in QD525 channel might also be attributed to "spectral leakage" contributed by cell autofluorescence, which is most pronounced in a blue-green spectral range. Scale bar, 50 $\mu$ m.



**Supplementary Figure S8. Preservation of the specimen morphology throughout 5 cycles of 5-color target re-staining with M3P technology.** The same set of 5 model molecular targets (from left to right, Ki-67, HSP90, Lamin A, Cox-4, and  $\beta$ -tubulin labeled with QD-SpA-Ab probes emitting at 525, 545, 565, 585, and 605 nm respectively) is re-stained through 5 cycles (**C1-C5**). Qualitative evaluation of individual QD channels (columns 1-5) as well as composite images (column 6) of the same cell sub-population imaged at low magnification after every cycle shows robust re-staining of each target with preserved specimen morphology. Note that complete specimen regeneration after each cycle leaves no detectable fluorescence signal (Supplementary Fig. S7) and ensures that observed staining is generated by incubation of cells with a new QD-SpA-Ab cocktail during each cycle. Scale bar, 250 $\mu$ m.